Lanthanide-Based Resonance Energy Transfer

Paul R. Selvin

(Invited Paper)

Abstract— **Fluorescence resonance energy transfer is a powerful tool for studying nanometer-scale distances in biological macromolecules under physiological conditions. Using luminescent lanthanides instead of conventional fluorophores as donor molecules in energy transfer measurements offers many technical advantages and opens up a wide-range of new applications. Lanthanide photophysics and the instrumentation underlying these advantages are discussed. One new application, the study of conformational changes in the large protein complex actomyosin, which is responsible for muscle contraction and subcellular movement in many eucaryotes, is briefly discussed.**

I. Introduction and Background

FLUORESCENCE resonance energy transfer (FRET) is a technique for measuring the distance between two points which are separated by approximately 10–80 Å. The technique is valuable because measurements can be made under physiological (or other) conditions with near-Angstrom resolution and with the exquisite sensitivity of fluorescence measurements. For these reasons FRET has found wide use in polymer science, biochemistry and structural biology. A number of reviews have been written [1]–[7]. More recently, we and others have introduced a modification of the standard technique, which we call luminescence (or lanthanide-based) resonance energy transfer (LRET). LRET offers many technical advantages over FRET, and yet relies on the same fundamental mechanism. We therefore begin with a discussion of the underlying theory and mechanism.

The idea behind resonance energy transfer is to label the two points of interest with different dyes, one, which must be fluorescent, is called the donor, and the other, which must have the appropriate absorption characteristics (and is often fluorescent as well, though not necessarily so) is called the acceptor. By choosing dyes with the appropriate spectral characteristics, the donor, after being excited by light, can transfer energy to the acceptor via an induced dipole-induced-dipole interaction. The efficiency of energy transfer depends on the inverse sixth power of the distance between the dyes. In general, the acceptor must be within 10–80 Å to get reasonable energy transfer, the exact range depending on the dyes chosen.

FRET achieves near Angstrom resolution while utilizing visible wavelength light because it relies on the near-field of two interacting molecules: the classical diffraction limit which limits resolution to $\sim\lambda/2$ is only relevant for the far-field. The donor is excited by the excitation light, loses some energy to internal vibrations, and produces an electric field which looks like an oscillating electric dipole field—decreasing as $1/R^3$—at distances much less than the wavelength of light. At distances much farther than λ, the electric field is a propagating field decreasing as $1/R$, and this far-field is just the emitted photons of the donor. The frequency of this donor-electric field is somewhat lower than the excitation light frequency because of energy loss in the donor due to phonons (vibrational modes) (see Fig. 1). In FRET, it is the near-field which is of interest since the donor and acceptor are separated by distances much less than λ. If an acceptor molecule is in the donor's near-field and has energy levels that correspond to the frequency of the donor's electric field, transitions will be induced in the acceptor, i.e., it will absorb energy from the donor field. The acceptor can then in turn transfer this energy into heat (nonradiative de-excitation), or emit photons at yet longer wavelengths (due to energy loss of vibrations in the acceptor).

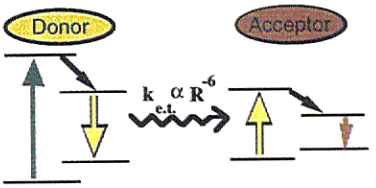

Fig. 1. Energy Diagram for FRET: The donor is excited, loses some energy due to internal vibration and then produces an electric field which leads to fluorescence or energy transfer to the acceptor if the acceptor is nearby (on the order of R_o or less) and has the appropriate energy levels. The acceptor loses some energy due to internal vibrations and then can re-emit at longer wavelengths. The internal vibration process is fast (picoseconds) compared to the other processes, preventing back-transfer of energy, and making the flow of energy unidirectional.

The Hamiltonian, or energy of interaction between the donor and acceptor is

$$H = \frac{\mu_D \cdot \mu_A}{R^3} - \frac{3(\mu_D \cdot \mathbf{R})(\mu_A \cdot \mathbf{R})}{R^5}. \tag{1}$$

$\mu_D(\mu_A)$ is the transition dipole moment of the donor (acceptor) and $\mathbf{R}$ is the vector separating their centers. According to Fermi's Golden Rule, the rate of inducing transitions is proportional to the square of the Hamiltonian matrix element between final and initial states

$$k_{et}\, \alpha \left[\langle D^* | \langle A | \frac{\mu_D \cdot \mu_A}{R^3} - \frac{3(\mu_D \cdot \mathbf{R})(\mu_A \cdot \mathbf{R})}{R^5} | D \rangle | A^* \rangle \right]^2 \tag{2}$$

Manuscript received November 5, 1996; revised December 23, 1996. This work was supported by National Institute of Health under Grant AR44420 and by the Office of Energy Research, Office of Health and Environmental Research of the Department of Energy under Contract DE AC03-76SF00098.

The author is with the Life Sciences Division, Lawrence Berkeley National Laboratory, Calvin Lab, Berkeley, CA 94720 USA.

Publisher Item Identifier S 1077-260X(96)09695-5.

where the initial state is the product of the excited state of the donor ($\langle D^*|$) and the ground state of the acceptor ($\langle A|$) and the final state is the product of the donor ground state ($|D\rangle$) and acceptor excited state ($|A^*\rangle$). The important point is that the rate of energy transfer depends on: the inverse-sixth power of the distance between the donor and acceptor; on their relative oscillator strengths—a larger donor oscillator produces a larger electric field and a larger acceptor oscillator is better able to take energy from the donor; on their relative orientation, as implied by the dot-products—if the transition dipole moment of the acceptor is not aligned with the polarization of the donor electric field, energy cannot be transferred; only those donor and acceptor states of similar energy will contribute to the energy transfer process—the resonance conditions of FRET.

The rate of decay of the donor excited state is just the sum of all decay rate pathways, $k_{nd} + k_{et}$ where k_{nd} is the sum of all distance-independent rates such as fluorescence (k_f) and heat (k_h), and k_{et} is the distant-dependent rate of energy transfer to the acceptor. The fraction of the donor's excited state energy (E, also called the efficiency of energy transfer) going to the acceptor is therefore just

$$E = \frac{k_{et}}{k_{et} + k_{nd}} = \frac{1}{1 + \frac{k_{nd}}{k_{et}}} \tag{3}$$

and

$$E = \frac{1}{1 + \frac{R^6}{R_o^6}} \tag{4}$$

or

$$R = R_o \left(\frac{1}{E} - 1 \right)^{1/6} \tag{5}$$

in which R_o is related to constants in k_{et} and k_{nd} and has dimensions of distance. From (4) it is easy to see that R_o is the distance at which 50% energy is transferred. R_o depends on the spectral properties of the donor and acceptor and is typically 10–55 Å for organic dyes, and up to 75 Å or longer when using lanthanides as donors. It can be shown [3] that

$$R_o = (8.79 \times 10^{-5} \ J q_D n^{-4} \kappa^2)^{1/6} \text{ (in Angstroms)} \tag{6}$$

$$J = \frac{\int \varepsilon_A(\lambda) f_D(\lambda) \lambda^4 \, d\lambda}{\int f_D(\lambda) \, d\lambda} \ (\text{in } \underline{\text{M}}^{-1} \cdot \text{cm}^{-1} \cdot \text{nm}^4) \tag{7}$$

where J is the normalized spectral overlap of the donor emission (f_D) and acceptor absorption (ε_A in units of $\underline{\text{M}}^{-1}$ cm^{-1} where $\underline{\text{M}}$ is units of Moles/l), q_D is the quantum efficiency (or quantum yield) for donor emission in the absence of acceptor (q_D = number of photons emitted divided by number of photons absorbed), n is the index of refraction (1.33 for water; 1.29 for many organic molecules) and κ^2 is a geometric factor related to the relative orientation of the transition dipoles of the donor and acceptor [the $\mu_D \cdot \mu_A$ term of (1)] and their relative orientation in space [the $(\mu_D \cdot \mathbf{R})(\mu_A \cdot \mathbf{R})$ term]. The expression for κ^2 is given in (8). κ^2 ranges from 0 if all angles are 90°, to 4 if all angles are zero degrees, and equals 2/3 if the donor and acceptor rapidly and completely rotate during the donor excited state lifetime [8]

$$\kappa^2 = (\cos \theta_{DA} - 3 \cos \theta_D \cos \theta_A)^2 \tag{8}$$

where θ_{DA} is the angle between the donor and acceptor transition dipole moments, θ_D (θ_A) is the angle between the donor (acceptor) transition dipole moment and the R vector joining the two dyes. The importance of the above equations [specifically (4) and (5), where (6)–(8) are defining equations] is that *energy transfer can be used as a spectroscopic ruler,* as first convincingly shown by Stryer and Haugland [9], i.e., one can determine distances by measuring the extent of energy transfer, assuming R_o is known (or more often) can be calculated from (6) and (7).

Energy transfer can be measured in a number of ways: by a decrease in donor fluorescence intensity (because some of the energy is going to the acceptor, instead of into fluorescent photons), by a decrease in donor excited state lifetime (because energy transfer to the acceptor is an additional relaxation pathway of the donor excited state), or more recently, by a decrease in donor photobleaching rate [10]–[12] (because the lifetime of the donor decreases with energy transfer, which decreases the probability of chemical reaction with the donor excited state, which leads to photobleaching); or by an increase in acceptor fluorescence. Measured via donor properties, the efficiency of energy transfer (E) is then

$$E = \left(1 - \frac{I_{D_A}}{I_D}\right) = 1 - \frac{\tau_{D_A}}{\tau_D} = 1 - \frac{\tau_D^{bl}}{\tau_{D_A}^{bl}} \tag{9}$$

where I_{D_A}, τ_{D_A}, and $\tau_{D_A}^{bl}$ are the donor's intensity, excited state lifetime, and photobleaching time constant in the presence of acceptor, resspectively, and I_D, τ_D, and τ_D^{bl} are the same parameters in the absence of acceptor. The extent of energy transfer can also be determined by measuring the increase in fluorescence of the acceptor due to energy transfer and comparing this to the residual donor emission:

$$E = \frac{\frac{I_{A_D}}{q_A}}{\frac{I_{D_A}}{q_D} + \frac{I_{A_D}}{q_A}} \tag{10}$$

where I_{D_A} is the integrated area under the donor emission curve in the presence of acceptor, I_{A_D} is the integrated area of the sensitized emission of the acceptor (i.e., not including the fluorescence due to direct excitation of the acceptor) and q_i is the quantum yield for donor or acceptor. The integrated areas are determined by curve fitting the spectrum to the sum of a donor-only and acceptor-only spectra. Qualitatively, this equation says that energy transfer takes area under the donor emission curve to area under the acceptor curve. Since E is defined in terms of *excitations,* not emissions, these areas are

normalized by their quantum yields, (which is just the ratio of emissions to excitations).

When measuring the sensitized emission of the acceptor and using (10), one must subtract out the component of acceptor fluorescence due to direct excitation and also subtract out donor emission which overlaps in wavelength with acceptor emission. This can be done by comparing multiple samples, labeled with donor-only, acceptor-only, and donor–acceptor. Clegg *et al.* have introduced an important method for making these subtractions on a single donor–acceptor sample, which greatly minimized errors due to concentration and labeling differences between such samples [13], [14]. Using lanthanides as donors eliminates the problem of subtracting out the direct acceptor fluorescence since the acceptor fluorescence is temporally discriminated against (see below) [15]–[18]. The importance of (10) is that it allows accurate measurement of relatively small amounts of energy transfer (distances $> R_o$). It is also interesting to note, though not widely appreciated, that by combining (5) and (10), the calculated distance is dependent only on the acceptor quantum yield. and not on the donor quantum yield:

$$R = C\left[\frac{I_{D_A}\, q_A}{I_{A_D}}\right]^{1/6} \tag{11}$$

where C is simply all the constants in R_o except q_D. This is advantageous since the quantum yields of organic dyes, which are used as acceptors, have been measured or can be measured straightforwardly, whereas, the lanthanide quantum yield is more difficult to measure directly (see below).

Lastly, we have recently shown that energy transfer between a single donor and single acceptor molecule can be measured [19]. E is measured either by changes in donor intensity before and after photobleaching of the acceptor, or by changes in the acceptor emission before and after the donor photobleaches. (see also Ha *et al.* this issue.)

II. Drawbacks of FRET

There are five main drawbacks of FRET.

1) The maximum distance that can be measured is less than optimal for many biological applications. The maximum distance measured in the literature is approximately 80 Å and at this distance the amount of energy transfer is very small and great care must be taken in the purification of the sample and in the measurement. The limited distance range is because of the relatively small R_o (i.e., fairly inefficient energy transfer), the sharp-drop-off in signal with distance, and the large amount of temporal and spectral overlap of donor and acceptor (i.e., large background). Many subcellular structures, however, are in the 80–130 Å range, including complexes such as membranes, protein-DNA complexes, and large proteins such as actomyosin.
2) Absolute distances are difficult to determine precisely because of uncertainty in the relative orientation of the two dyes, as expressed in the κ^2 factor. Uncertainty in κ^2 can often be reduced by showing that the dyes have rotational motion during their excited state lifetime, but rarely does this eliminate all uncertainty and the uncertainty is application specific. Indeed, for this reason, *FRET is most commonly used as a measure of relative distance.* (For example, the donor and acceptor are closer under condition A rather than condition B, where it is assumed that distance, and not relative orientation of the dyes changes with condition.)
3) The lifetime of commonly used donor fluorophores are short (typically a few nanoseconds) and are often multiexponential, making lifetime measurements difficult and of limited accuracy. An accuracy of 10% (which is in-fact difficult to achieve) limits measurements of quenching of more than 10% and hence less than $1.45R_o$. For R_o of 40–55 Å, the largest yet attained for small organic dyes, the maximum measurable distance via donor quenching is therefore 58–80 Å. Advances in lifetime measurements, particularly by the phase-modulation method where very good time-resolution can be achieved may become important in this area [20].
4) When measuring the sensitized emission of acceptor, the signal to background is poor, typically on the order of 1:1. The background arises from interfering fluorescence from the donor and from direct excitation of the acceptor by the laser or excitation light. The poor signal to background limits the maximum measurable distance and also makes measurement of the lifetime of the sensitized emission not feasible. The large background also severely inhibits the use of FRET on biological systems that are impure (where, for example, only a small percentage of donor–acceptor complexes form), or when the ratio of donor to acceptor is unknown. (Note that in some cases there are excellent ways of subtracting out this background [13], making the signal to noise significantly greater than than signal to background.)
5) The measurement and interpretation of FRET often requires the sample to be labeled and purified such that it has one donor and one acceptor, or at least that the extent of labeling is known. This is because donor and acceptor both contribute to background photons, and their contribution must be subtracted off if E is to be measured. In addition, any incomplete labeling by acceptor leads to a fraction of unquenched donor and an apparent decrease in E. However, there are many biological systems where such purity cannot be achieved.

III. LRET Overcomes Problems of FRET and Enables New Applications

We and others have recently introduced LRET, an extension of FRET, in which the donor is a luminescent lanthanide chelate [5], [15]–[18], and the acceptor is a standard organic dye. Emission from lanthanides arise from high-spin to high-spin ($4f \rightarrow 4f$; see below) transitions, and hence technically should not be called fluorescence (which is emission from singlet-to-singlet transitions). Good reviews of lanthanide luminescence have been published [21], [22]. One

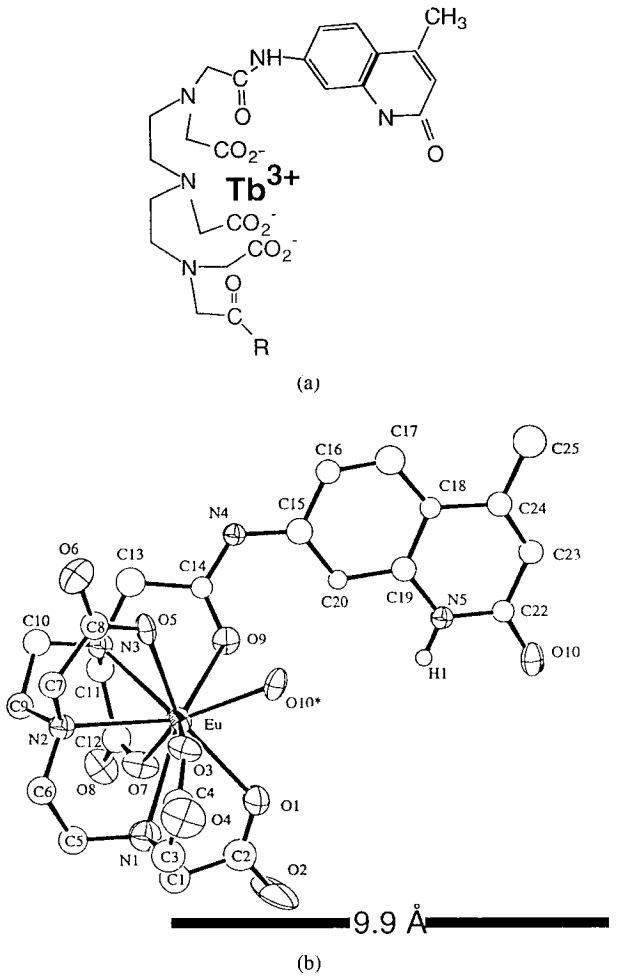

Fig. 2. DTPA chelate of terbium or europium with sensitizer (carbostyril 124) and its crystal structure. The R-group is one or several reaction groups for attachment to macromolecules (not present in crystal structure). The complex is roughly 12.8 Å × 8.1 Å × 8.3 Å, which is comparable to many organic fluorophores. In solution, the last coordination site (O10*) is occupied by a water molecule. Crystal structure adapted from [44]

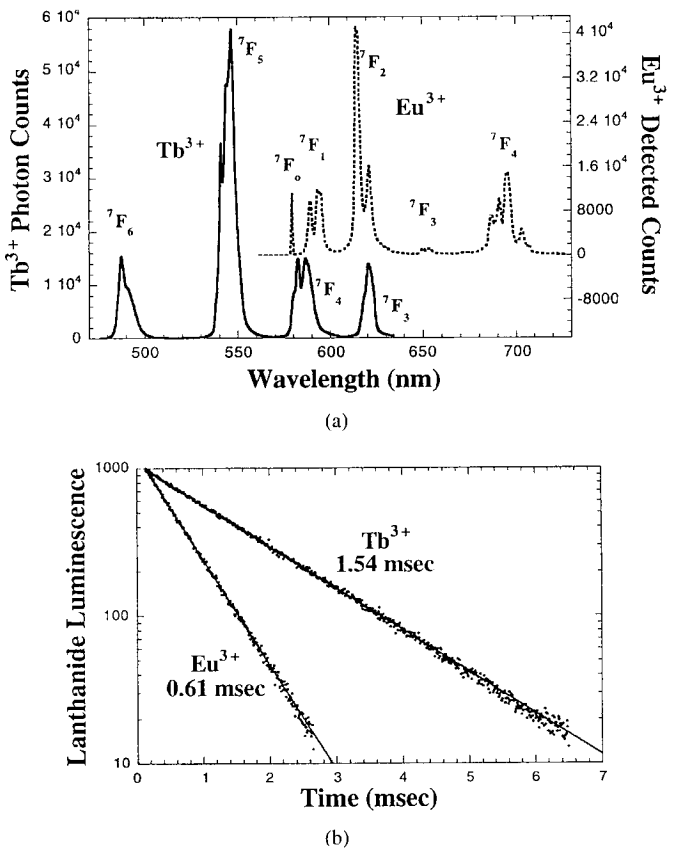

Fig. 3. (a) Emission spectra and (b) excited state lifetime of Tb^{3+}—and Eu^{3+}—DTPA-cs124 in H_2O at pH 7.0. For emission spectra [Tb^{3+}] at 0.25 μM and Eu^{3+} at 2 μM. Spectral data acquired with CCD integrated for 3 seconds with 600 g/mm grating, entrance slit of 0.1 mm, chopper delay of 145 μs. Excitation is approximately 5 μJ/pulse, 40-Hz pulse-rate at 337 nm (see instrumentation section, below). Lifetime measurements acquired in 10 s and normalized.

particular chelate, Diethylenetriaminepentaacetic acid (DTPA) covalently attached to the organic chromophore, carbostyril 124 (cs124), is shown in Fig. 2. Both terbium and europium are luminescent in this complex, and the emission spectra and excited-state lifetimes of Tb^{3+} and Eu^{3+} in this chelate are shown in Fig. 3. (Other oxidation states of Tb and Eu are only very weakly luminescence, if at all.) We have synthesized a number of other chelates, some of which are better than DTPA [23], and have also synthesized a number of different amine- [24] and thiol-reactive [25] forms for attachment to biomacromolecules. Others have used europium-cryptates as energy transfer donors [17], [18].

The chelate serves several purposes. It: 1) binds the lanthanide extremely tightly ($K \gg 10^{14}$ M^{-1} [23] where K is the binding constant of the chelate for Tb^{3+} or Eu^{3+}), 2) removes water molecules from the lanthanide primary coordination sphere, which can quench luminescence [26], leaving either zero or one water molecule out of a possible nine [23], 3) enables site-specific attachment to macromolecules, and 4) enables covalent attachment of a "sensitizer" or "antenna" molecule (cs124) which absorbs excitation light and transfer energy to the lanthanide, thereby overcoming the inherently weak absorption of the bare lanthanide ($\varepsilon_{\mathrm{Tb\,or\,Eu}} \approx 1\ M^{-1} \cdot cm^{-1}$; $\varepsilon_{\mathrm{cs124}} = 12\,000\ M^{-1} \cdot cm^{-1}$).

The lanthanide emission characteristics in such chelates are highly unusual: 1) The lanthanide quantum yield is likely near unity in D_2O because luminescence arises from inner shell electrons ($4f \rightarrow 4f$) which are isolated from the solvent by the chelate and because the chelate itself does not contain vibrational modes capable of deexciting Tb or Eu excited states ([15] and references therein). In H_2O the quantum yield can still be very high because the chelate removes H_2O molecules from the primary coordination sphere. Assuming the lanthanide quantum yield is unity in D_2O, the quantum yield drops to $\xi/(n\tau_{D_2O} + \xi)$ where ξ is a constant (1.05 for Eu and 2.42 for Tb), n is the number of H_2O molecules in the primary coordination sphere, and τ_{D_2O} is the lanthanide excited state lifetime in D_2O [23]. For DTPA in H_2O, the quantum yield for Eu is 0.26 and for Tb it is 0.6. 2) The emission is likely unpolarized. 3) The emission is sharply spiked with peak-widths of <5 nm full-width at half-maximum (FWHM) , and other regions which are dark. 4) The excited state lifetime is ≈ millisecond. (Tb lifetime of DTPA-cs124 complex in H_2O and D_2O = 1.5 and 2.6 ms, respectively; Eu lifetime, 0.62 and 2.5 ms.)

We and others have shown that these characteristics are highly advantageous for resonance energy transfer studies [15]–[18], [23]. The sharply spiked emission yields excellent spectral overlap with suitable acceptors ($J \approx 10^{16}\ M^{-1} \cdot cm^{-1}nm^4$); the high quantum yield and spectral overlap yields large R_o (>70 Å [15]–[18], [23]); the unpolarized emission constrains κ^2 to be $1/3 < \kappa^2 < 4/3$ because the donor is effectively randomized, even if stationary; the sensitized emission of the acceptor can be measured with no background from donor emission, which is spectrally eliminated, and no background from direct acceptor emission, which is temporally eliminated.

These characteristics have important implications in energy transfer measurements. 1) The large R_o yields strong energy transfer even at relatively large distances. 2) The long donor-lifetime means it is easy to measure donor lifetime quenching which is generally more accurate and less sensitive to artifacts than donor-intensity measurements. In addition, because the donor lifetime is generally single exponential in the donor-only complex, multiple donor–acceptor species containing different transfer efficiencies can be deduced and measured because they lead to a multi-exponential donor decay. 3) The ability to discriminate against background when measuring sensitized emission results in an improvement in signal to background of a 100-fold over organic dye-based FRET. Because background is now so low, small signals can be measured, corresponding to relatively large distances. Indeed, by a dark-background sensitized emission experiment, Horrocks and co-workers have shown the ability to measure distances at $4R_o$, although their R_o was only 3 Å [27]. However the R_o when using lanthanides as donors can be 70 Å or more, and the same dark-background holds, potentially enabling measurements of 100–200 Å. Equation (10) can also be used without the need to subtract off the direct emission, lending yet greater accuracy to energy transfer measurements on distances much beyond R_o. 4) Because donor-only and acceptor-only species do not contribute to background, measurement of energy transfer in a donor–acceptor complex can be done in the presence of donor-only and acceptor-only complexes. This minimizes the need for purification or isolation of the doubly labeled donor–acceptor complex from singly labeled (donor-only or acceptor-only) complex, and makes it possible to measure energy transfer on systems where the ratio of donor to acceptor is not—or cannot be—determined. 5) We have also shown the lifetime of the sensitized emission can be measured, which has all the advantages of an intensity measurement, but is insensitive to concentration, as well. In addition, by comparing the lifetime(s) of the sensitized emission (sensitive only to donor–acceptor complexes) with that of the donor lifetime (sensitive to all donor-containing complexes) one can get information about inhomogeneity—if the two lifetimes are not equal, then there is a spectrum of donor–acceptor transfer efficiencies. 6) Finally, because lanthanide emission is likely unpolarized (see below), one can assume $\kappa^2 = 2/3$, leading to at most an 11% error in the derived distance due to orientation of the acceptor. If the acceptor has some rotational mobility, this error decreases. Consequently, by knowing the parameters which determine R_o, it may now become possible to measure absolute distances via energy transfer.

We have previously published results which demonstrate LRET on DNA of well defined geometry [5], [15], [16], [24]. One such data set is shown below, where europium transfers energy to Cy5 [16]. A DNA oligomer, 10 bases in length, was labeled with Eu-DTPA-cs124 at one end, and a complementary DNA oligomer, which hybridizes, or binds to the other piece, was labeled with the acceptor Cy5 [Fig. 4(a)]. A mixture of donor–acceptor complex and donor-only complex was made to demonstrate the ability to detect different species. The donor lifetime (at 616 nm) of the mixture is bi-exponential, with the long-time component corresponding to the single-stranded, unquenched donor DNA, and the short-time component corresponding to the hybridized donor—acceptor complex [Fig. 4(c)]. The sensitized emission of the acceptor (at 668 nm) can isolate the signal from the donor–acceptor complex even in the presence of donor-only and acceptor-only species. (The donor-only signal is eliminated spectrally, the acceptor-only signal eliminated temporally. The 59-μs component at 668 nm is due to detector ringing caused by the prompt acceptor fluorescence and is not physically significant.) A signal-to-background of approximately 90:1 [Fig. 4(b)] is measured for the sensitized emission intensity after a 150-μs delay, roughly a 50–100 times improvement over the same measurement using conventional dyes.

The main limitation of LRET is that it requires relatively low-noise detectors (see instrumentation section below) and that the long-lifetime of the lanthanides means that intermolecular/diffusional energy transfer can occur. Indeed, lanthanides were first used in energy transfer experiments to determine rates of diffusion and contact distances [28]. It is therefore imperative to measure energy transfer at several different concentrations, to ensure that diffusional energy transfer is not significant. This problem obviously becomes more severe as the macromolecules become smaller and therefore diffuse faster, and as the amount of intra-molecular energy transfer one wishes to measure gets smaller. With relatively small molecules such as 10–20 base-pair DNA oligomers, we found that at concentrations of 0.25 μM or less, intermolecular energy transfer was less than a few percent [15], [16]. If necessary, intermolecular diffusional energy transfer can be reduced by increasing the viscosity of the solution (sucrose often works well; glycerol is another possibility), if this does not interfere with biological function or structure.

IV. Instrumentation

One of the advantages of using lanthanides is that because of their millisecond lifetime, time-resolved instrumentation is fairly simple. However, off-setting this is the fact that lanthanide emission is quite weak, and hence low-level detectors are highly desirable. The weak emission intensity of lanthanides is inherent: A molecule with a millisecond lifetime can emit at most 1000 photons per second per molecules, whereas conventional fluorophores, which typically have 1–10 ns lifetime, can emit 10^8–10^9 photons/s/molecule, although

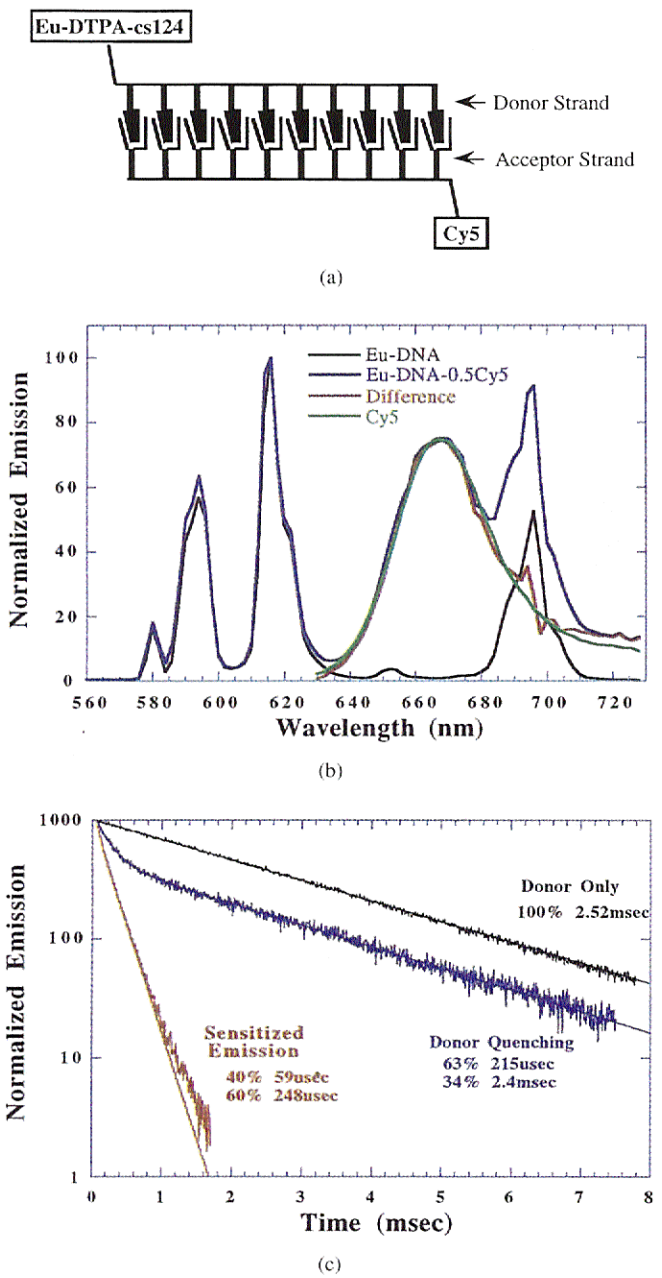

Fig. 4. (a) Schematic of model system used for energy transfer, (b) emission spectra after 150-μs delay time showing enhanced acceptor emission (sensitized emission) due to energy transfer, and (c) excited state lifetime of donor and sensitized emission, showing bi-exponential donor lifetime (at 617 nm) due to mixture of donor-only and donor–acceptor complex and primarily single exponential sensitized emission of acceptor (at 668 nm; 59-μs component due to ringing of detector from prompt acceptor fluorescence) due only to the donor–acceptor complex in the mixture.

emission rates of 10^4–10^5 are more common. In addition, the effective absorption cross section of conventional dyes is often a factor of 10 higher. These factors make the use of lanthanide in microscopy (particularly scanning microscopy), problematic, especially when few molecules are present and rapid data acquisition may be important. However, in cases where background autofluorescence obscures the signal when using conventional fluorophores, and when many lanthanide chelates can be attached to the object of interest, dramatic improvements—up to 400-fold—in signal to background can be achieved by replacing organic fluorophores with lanthanide complexes [29], [30]. Since the lanthanides do not, in general, self-quench [31]–[33], signal can be improved by addition of a large number of closely spaced luminescent lanthanide chelates. For energy transfer measurements in a microscope, it should in some cases be possible to use many lanthanide donors with a single organic-based acceptor, since one acceptor can quench hundreds of lanthanides without saturating.

For energy-transfer measurements, we have built a time-resolved spectrometer capable of both time-resolved measurements at a single wavelength, and integrated measurements at many wavelengths simultaneously. The excitation source is a nitrogen laser (Laser Photonics, Orlando FL: 337-nm 40-Hz 7-mW average power, 5-ns pulsewidth). Two mirrors are used to rotate the rectangular laser-beam profile so that the larger dimension is vertical. After passing through a neutral density filter and slit, the power after the sample cuvette (typically 5–10 μJ per pulse) is monitored via a power meter (Molectron, Portland, OR, Model J4-09 with JD1000 display). 20–200 μL of sample solution is placed in a 2 mm $\times$ 2 mm or 3 mm $\times$ 3 mm (i.d.) quartz cuvette and the emission detected at right angles with a high numerical aperture lense. The emission light is then f-matched to the spectrometer (SPEX 270M, $f/4$, with dual exit port) with a second lense and focused onto the side entrance slit. A mechanical chopper (Stanford Research System, Palo Alto, CA, model SR540) with a modified chopper-blade is placed as close as possible to the side-entrance slit. (Space-constraints prevent the front entrance slit of the spectrometer from being used with a chopper.) The chopper is timed (see below) such that the entrance slit is blocked during and immediately after the laser pulse to eliminate prompt fluorescence of the acceptor and any other short-lived background such as Raman of water. The sample fluorescence/luminescence is detected either with a water-cooled photon-counting photomultiplier tube (Hamamtsu R298-04; gallium arsenide photocathode with Products for Research TE104 cooling housing and PMT resistor chain) or a liquid-nitrogen cooled CCD (SPEX Spectrum One: 1024 $\times$ 256 27-μm pixels, front illuminated 16-b digitization; noise: 1e/h/pixel; readout-noise <5 electrons). A computer-controlled moveable mirror inside the spectrometer directs the light to either (but not both simultaneously) of the detectors. The output of the PMT is discriminated and amplified by a Hamamtsu C3866 preamplifier/discriminator and the resulting TTL pulses are counted in a multichannel scalar with 2 μs resolution (Canberra FMS pc-board; an EG&G MCS-Plus has also been used). Because of memory incompatibilities between the CCD and the multichannel scalars board, they were placed in different pc-compatible (486 or Pentium-based) computers.

Timing of signals is done by using the chopper TTL output and two pulse generators (Stanford Research System DG535). When using the CCD as detector, the "f" TTL output of the SRS chopper is used as the master clock. (The "f" output is actually at six times the rotation frequency of the wheel since the original wheel has 6 blades.) By triggering the laser with an output derived from this source, any jitter in the chopper wheel is inconsequential. The chopper is set to a near-maximum

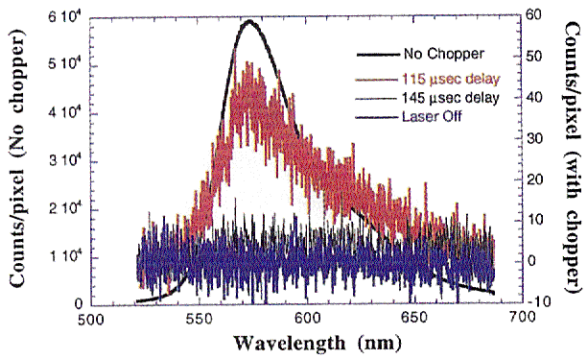

Fig. 5. Tetramethylrhodamine fluorescence as a function of chopper delay setting. Direct fluorescence of the acceptor (here TMR) can be eliminated by placing a chopper in front of the entrance slit of a spectrometer equipped with a CCD detector. The chopper frequency is 79.6 Hz and the slit is uncovered a given delay time after the laser is fired. The delay values correspond to the time after the pulse that a steady-state signal has reached 90% of its maximum. The 50% point is reached 25 μs earlier than the 90% time. A delay of 115 μs yielded a 2000-fold rejection of direct fluorescence; a delay of 145 μs yielded greater than 25 000-fold rejection. The CCD integration time was 4 s except for data at 145 μs delay, which was 16 s. The average of the laser-off data was subtracted from all data to eliminate the constant (noise-free) offset of the CCD output. An entrance slit width of 0.1 mm and a 600 groove/mm diffraction grating blazed at 550 nm was used. TMR concentration was 1.6 μM.

rotation rate of 478/6 = 79.66 Hz to minimize dead-time. The TTL output of the chopper triggers pulse generator #1, which serves to down-convert the pulse rate to 40 Hz, the maximum laser repetition rate. (One of the outputs is set to trigger + 0.024 95 s, disabling all outputs until this has clocked out.) An output from pulse generator #1 (20-μs pulse from the "A–B" output with no delay after the trigger from chopper) then triggers a second pulse generator. The "A" output of generator #2 is set a variable delay time after the trigger and is used to trigger the MCA. A second output from pulse generator #2 sends a 10-μs pulse to trigger the laser, 30 μs after the "A" output. Hence, the MCA is always triggered 30 μs before the laser, which is triggered a variable delay time after the pulse from the chopper. This delay is determined by exciting a solution containing a prompt fluorophore (such as tetramethylrhodamine [TMR]) and setting the delay to optimize the discrimination against prompt fluorescence while minimizing the dead-time (the time when the slit is covered by the chopper blade) after the laser pulse (see Fig. 5).

To acquire data when using the CCD, the chopper is turned on and pulse generator #2 is set to external mode, which starts the laser firing. The CCD acquire-button is immediately pressed and integration occurs for the computer-preset time. To acquire data when using the PMT, the chopper is turned off with the entrance slit uncovered, and generator #2 is used as the master clock (internal triggering mode). The dead-time when using the chopper can be determined trivially by using a steady-state light source (such as a flashlight) with the chopper running and the PMT/MCA as the detector.

V. Measuring Distances Beyond R_o

When attempting to measure distances much beyond R_o, where energy transfer efficiencies are a few percent or less, there are a number of experimental issues which must be addressed. The first issue that must be addressed is insuring that the detected energy transfer is due to intramolecular energy transfer, and not diffusional energy transfer. Depending on the size of the macromolecules being examined, this may necessitate dilute solutions, which may or may not be possible, depending on the stability of biological assemblies. Dilute concentrations can also potentially lead to low signal levels, making low-noise detectors, efficient collection of emitted light, and bright lanthanide chelates (see Tb versus Eu, below) important.

When measuring distances out to approximately $1.5R_o$ ($E = 10\%$), donor lifetime measurements can be made, since donor lifetimes can in general be made with a precision of a few percent. However, at distances greater than this, one must measure energy transfer by (10). Large distances can be measured because one can very accurately fit curve-shaped, especially when using a CCD, in which all wavelengths are captured at once, eliminating any error in line-shape due to excitation intensity fluctuations or photobleaching during an acquisition period. (When using a CCD, if the donor photobleaches during an acquisition, all signal goes away, and there is no effect on E; if, however, the acceptor photobleaches during the acquisition and stops absorbing, then E measured via (10) will be the time-average of E before photobleaching and $E = 0$ after photobleaching.) However, it is important that any area under the acceptor emission curve be due only to energy transfer. Hence, it is critical to eliminate all direct acceptor emission, and using a chopper achieves this quite well (Fig. 5). Emission from the acceptor even after the time-delay, however, can arise from inner-filter effect—the trivial reabsorption of a donor photon by the acceptor due to finite optical thickness of the sample. The absorbance at the donor-emission wavelength due to the acceptor must therefore be significantly below the fraction of energy transfer being measured, or if not, then the contribution due to inner-filter effect must be accurately known and subtracted out. This again, may necessitate dilute samples or thin samples. For this purpose, a microscope objective, with its efficient collection of light and shallow depth of field is ideal.

While (10) can be used to measure small amounts of energy transfer, measuring the sensitized emission lifetime is very difficult at large distances due to limited photon flux. When measuring lifetimes (as opposed to intensities), one inherently divides the signal into time-bins, making the total number of photons collected for reasonable statistics significantly larger. In addition, in order to eliminate donor-emission, one must collect the sensitized emission with a bandwidth of only a few nanometers, further decreasing signal level. For example: if one is trying to measure 10% energy transfer, the signal intensity of the acceptor will be 0.1 $\times q_A \times$ (BW/FW) where BW is the bandwidth of detection and FW is the full-width of the acceptor emission. With BW = 2 nm, and FW = 50 nm, and a q_A of 0.2 (the approximate quantum yield of many organic acceptors), the acceptor signal is a factor of over 1250 less than the donor signal. If one needs to measure the sensitized emission lifetime at relatively large distances, using the relatively large dark-region of Tb around 516 nm and a high quantum yield acceptor like fluorescein (which absorbs at

the 492-nm Tb emission line), can help increase the sensitized emission signal significantly (although at a cost of smaller R_o as compared to using the 546-nm line of Tb). (Such a situation might arise if the labeling and isolation of the donor–acceptor complex is difficult, leaving a large amount of donor-only and acceptor-only complexes—the sensitized emission lifetime signal arises only from the donor–acceptor complex.)

VI. Lanthanide Photophysics

Here we discuss some of the detailed photophysical questions pertinent to lanthanides in resonance energy transfer.

- Is the dipole-dipole theory of Förster applicable?

Emission of lanthanides arise from $4f - 4f$ inner shell electrons, a transition which is formally parity forbidden via electric-dipole transitions. Indeed, magnetic dipole and electric quadrupole transitions in lanthanides have been observed [34], and Dexter, in his seminal paper [35], showed that these transitions are ineffective at transferring energy to an electric-dipole acceptor. In contrast, all emission arising from organic fluorophores are from electric-dipole transitions. Since Förster's theory depends on an electric-dipole-electric dipole interaction, it is *a priori,* unclear that lanthanides obey this theory which underlines FRET.

It has been shown, however, that most emission from lanthanides in solution comes from "forced" electric-dipole transitions arising from an admixture of odd-parity states ($5d$-states) into the $4f$ emission levels. Hence, the electric field arising from these transitions is electric dipole in nature and the underlying Förster theory is applicable. The maximum electric field strength produced by the lanthanide is lower than that produced by an organic fluorophore, by the square-root of their lifetimes (roughly [ms/10 ns]$^{1/2}$, or 300-fold less), but the efficiency of energy transfer depends only on the relative rate of energy transfer to the acceptor versus the rate of deactivation of the donor excited state via other pathways (3). As long as the latter is small compared to the former, energy transfer efficiency will be high. However, two important subtleties exist. First, there can be significant magnetic dipole transitions, and these transitions cannot transfer significant energy to a conventional (electric-dipole) acceptor. Hence, when calculating the spectral overlap term (J) in (7), one must include only those emission lines which are due to electric dipole transitions. In the case of europium, it is known that the $^5D_0 \rightarrow {}^7F_2$ transition (≈580–595 nm) is magnetic dipole, and so must be excluded in the overlap integral of (7). The photophysics of terbium is considerably more complex than europium (see below: Tb versus Eu), and the exact nature of each transition is not well known, although it is possible that the main Tb^{3+} emission of $^5D_4 \rightarrow {}^7F_5$ (≈546 nm) contains some magnetic dipole character. Any MD character serves to reduce the effective R_o. The second complication has to due with the definition of the quantum yield term (q_D) in (6). This is discussed in more detail below, but the conclusion is that as long as one uses the lanthanide quantum yield, and not the "overall" quantum yield of the chelate, Förster's theory is completely and rigorously applicable to lanthanide-based resonance energy transfer.

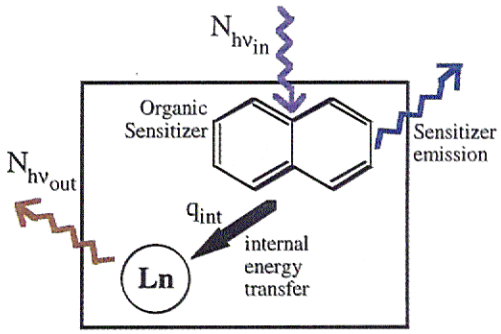

Fig. 6. The "overall" quantum yield is $N_{h\nu_{\rm out}}/N_{h\nu_{\rm in}}$, where $N_{h\nu_{\rm in}}$ is the number of absorbed photons, and $N_{h\nu_{\rm out}}$ is the number of photons emitted by the lanthanide. The sensitizer emission is of little interest and is not relevant in LRET except to the extent it is a competitive pathway for energy flow from the sensitizer to the lanthanide and therefore decreases overall lanthanide emission. The lanthanide quantum yield is the overall quantum yield times $q_{\rm int}$ (see also text).

- What is meant by quantum yield?

Quantum yield is defined as the total number of emitted (fluorescent or luminescent) photons divided by the total number of excitation photons absorbed. The quantum yield therefore varies between zero and one. For organic fluorophores, in which the absorbing and emitting molecule is the same, the definition is unambiguous. However, for complex compounds such as the lanthanide chelates, which contain an absorbing (organic) chromophore and a separate emitting object (the lanthanide), there are two different "quantum yields" which are commonly referred to (Fig. 6). We distinguish these two by "overall quantum yield" ($q_{\rm all}$) and by "lanthanide quantum yield" (q_{Ln}). $Q_{\rm all}$ treats the chelate-complex as a "black-box" and is the number of photons emitted by the lanthanide divided by the number of photons absorbed by the sensitizer. (The total absorption is technically the absorption of the lanthanide plus sensitizer, but the former is negligible. The total emission is technically the emission of the lanthanide plus emission of the sensitizer, but emission of the sensitizer is rarely of any interest, and so is neglected.) Q_{Ln} is defined as the number of emitted lanthanide photons divided by the number of quanta absorbed by the lanthanide. The two are directly related by

$$q_{\rm all} = q_{Ln} \times q_{\rm int}$$

where $q_{\rm int}$ is the number of quanta of energy transferred from the sensitizer to the lanthanide, divided by the number of quanta absorbed by the sensitizer. $q_{\rm int}$ is the quantum yield for energy transfer from the sensitizer to the lanthanide.

The overall quantum yield is relevant to the overall brightness of the chelate-complex but is of only secondary interest in resonance energy transfer measurements. It is relevant only to the extent that the total number of photons may limit the signal to noise. In contrast, it is the "lanthanide quantum yield" which is central to resonance energy transfer measurements. $q_{\rm Ln}$ is the value that must be used in Förster's theory to determine R_o. $q_{\rm Ln}$ relates the relative rates of radiative and nonradiative de-excitation of the lanthanide, and it is these relative rates, or efficiencies, which determine R_o and E in (6) and (3), respectively. The main determinant of $q_{\rm Ln}$ is the number of waters bound to the primary coordination sphere of

the lanthanide, as discussed previously, although vibrational modes of the chelate and of the sensitizer can potentially deexcite the lanthanide excited state. In polyaminocarboxylate chelates in D_2O, it is likely that q_{Ln} is very high—near unity. (See discussion of R_o, below, for further discussion of this unity assumption.) In contrast, the q_{int} is on the order of 0.2 for cs124 to Tb and less for cs124 to Eu, making $q_{all} < 0.2$.

Rather than thinking of q_{int} affecting the quantum yield of the chelate, it is more accurate, in the context of resonance energy transfer, to think of it as affecting the effective absorption of the chelate, which has no effect on R_o. The effective absorption of the lanthanide is just the absorption cross section of the sensitizer ($\varepsilon_{sensitizer}$) times q_{int}

$$\varepsilon_{effective} = \varepsilon_{sensitizer} \times q_{int}.$$

There is one final complication in discussing quantum yields. In resonance energy transfer it is actually the lanthanide quantum yield for electric dipole emission ($q_{Ln\text{-}ED}$) which is important, since any MD transitions do not contribute to energy transfer. ($q_{Ln} = q_{Ln\text{-}ED} + q_{Ln\text{-}MD}$). However, since the fraction of ED versus MD is wavelength dependent, it is better to include this effect in calculating J: the f_D in the J integral in (7) is defined to include only those photons which arise from ED transitions.

- What is κ^2?

When using lanthanides as donors, there are two factors which greatly limit the uncertainty in κ^2: the long lifetime, and the multiple transition dipole moments at different orientations. The long lifetime means that it is likely that the donor and acceptor will rotate during the donor's excited state lifetime, bringing κ^2 to 2/3. Even if the donor and acceptor are completely rotationally immobile, however, the fact that the lanthanide emits with multiple transition dipole moments [m_j values—see Fig. 3(a)], means that in-effect, the polarization of the donor's electric field is nearly-isotropic and equivalent to a rapidly rotating donor. For terbium, with each transition arising from highly degenerate states [$J = 4(^5D_4)$ to a $J =$ 0–6 (^7F_J)] the assumption of multiple dipole moments at many different orientations—and hence isotropic emission—is likely justified. For Eu, the excited state has $J = 0$ and so the number of transition dipole orientations is less, although the ground states of $J = 3$ ($^7F_3$) and $J = 5$ ($^7F_3$), which are the transitions of most interest in energy transfer, the number of transition dipoles $(2J+1)$ is still fairly large. If the donor emission is isotropic, either due to rotation within the millisecond lifetime, or due to multiple dipole moments, then $1/3 < \kappa^2 < 4/3$ and the uncertainty in the calculated distance due to uncertainty in the orientation factor is at worst 12%. Since the acceptor is rarely completely rigid on a millisecond-time scale, the uncertainty in distance is actually less than this, which opens up the possibility of measuring absolute distances via LRET, instead of simply relative distance measurements more often achieved in FRET.

- What lanthanide to use: Tb versus Eu?

At present, terbium or europium are the two practical lanthanides which can be used advantageously in energy transfer measurements. All lanthanides have very weak absorption cross sections, and hence require an antenna or sensitizer (cs124 in our case) which can facilitate lanthanide excitation at reasonable power levels. Some lanthanides, such as Gd^{3+}, cannot be used because sensitizers with the appropriate energy would require excitation in the deep ultraviolet [22]. It is also important that the lanthanide have a high quantum yield for emission when bound in a chelate in solution: only Tb and Eu presently meet this criteria [22].

In general, there are not large differences between terbium versus europium as donors. However, there are some subtle differences which can make one or the other more advantageous in particular circumstances. A quick summary: The maximum R_o achievable is similar for the two lanthanides, although potentially somewhat larger with Eu; in the current generation of lanthanide chelates we have developed, terbium is brighter (i.e., more photons emitted for the same excitation level), which can be important for measuring large distances on dilute samples, but terbium photophysics is less well characterized.

R_o: R_o is dependent on a number of factors, as described in (6). When looking at large distances, a large R_o is highly desirable. For shorter distances, R_o can always be reduced by choosing acceptors with less spectral overlap or using chelates in which the lanthanide has a lower quantum yield due to bound waters. The maximum spectral overlap, and hence largest R_o is currently achieved when using carbocyanine dyes [36], [37] as acceptors. In H_2O (D_2O), Tb-DTPA-cs124 to Cy3 has an R_o of 64 Å (70 Å), and Eu-DTPA-cs124 to Cy5 has an R_o of 56 Å (70 Å). With other chelates that either concentrate the europium emission into a single band where the acceptor absorbs, or which accentuates the long-wavelength europium emission [see (7) and note the λ^4 dependence in J), R_o can increase to as much as 68.6 Å in H_2O and 76 Å in D_2O with carbocyanine acceptors [23]. A hypothetical carbocyanine dye which had an absorption spectra of Cy5 but blue-shifted 34 nm (so the absorption maximum of the dye matches the 616 nm Eu line) would increase R_o with Eu-DTPA-cs124 to 80 Å in D_2O (64 Å in H_2O) and with Eu-TTHA-cs124 to 85.5 Å (80 Å in H_2O) (see [23] for the structure of TTHA).

These R_o values assume all emission is electric dipole, except for the known MD-transition of $^5D_o \rightarrow {}^7F_2$ (≈590–600 nm) in Eu, and that the quantum yield is unity in the chelates in D_2O. As previously mentioned, the assumption of complete ED character may not be rigorously correct, especially for the 546 nm line of Tb. The extent of ED versus MD may also depend on chelate symmetry, with symmetric chelates enhancing MD character. Experiments to determine the fraction of ED versus MD character can be made on single crystals, and are currently underway for Eu-DTPA-cs124. However, the R_o is probably not in error by a great amount because the above assumption yields distances which are consistent with known dimensions. (For measurements on DNA, see [15], [16]; for measurements on the protein myosin, see below.) In addition, in previously published work [15], we had implicitly assumed that the quantum yield for electric dipole emission in Tb-DTPA-cs124 in D_2O was unity (see [15, eq. (1)] and compare

to (10) here). Using this assumption we had calculated q_A, and found results which were in reasonable agreement with standard methods of measuring q_A.

VII. Applications

A. Muscle

Muscle contraction and a variety of subcellular motion in eucaryotes (cells with nuclei) is caused by the interaction of two proteins, myosin and actin. (For a general reference, see [38].) Each protein polymerizes to form filaments, and it is the relative sliding of these filaments with respect to each other which leads to muscle contraction and motion (see Fig. 7). Protruding from the thick filament are myosin "heads" or crossbridges, which attach to the thin filament, undergo a conformational change, and pull the filaments past each other. This model is often called the "tilting oar" or "swinging crossbridge" model of muscle mechanics because the myosin head is thought to act like an oar, undergoing a rotation or "powerstroke" that sweeps the thin filament past the thick filament. The energy for this work is derived from the chemical compound ATP (adenosine triphosphate). Although much indirect evidence supports this "tilting oar" hypothesis, after decades of work, the direct visualization of the force-generating powerstroke has yet to be achieved. It is now known that in each power-stroke, actin is translated with respect to the myosin $\approx$5 nm [39] and that conformational changes within the myosin head are sufficient to produce this motion. The myosin head contains two parts, the catalytic domain, which is believed to remain strongly bound to the actin during the powerstroke, and a neck region, which is believed to undergo a roughly 40° rotation during the powerstroke (see Fig. 7). (Despite the confusing terminology, the "neck" region is part of the myosin "head.") The net effect is a translation of the actin filament (see figure). Irving *et al.* recently used fluorescence depolarization of a fluorophore attached to the myosin neck and found an average rotation of 3° during the powerstroke [40], [41]. This important result supports the tilting oar hypothesis, but to achieve the 5-nm relative motion which is believed to occur during the power-stroke, closer to a 40° rotation is expected.

FRET has been used extensively to investigate conformational changes in myosin (reviewed in [42]), but has failed to provide definitive answers, particularly to the question of distances between sites on myosin and actin, mainly because of the drawbacks cited earlier. Below we show that LRET is capable of making the relatively long-distance measurements necessary on this rather complex molecule. Future publications will discuss experimental details and changes in distances (manuscript submitted). A terbium donor was placed on the neck region (the regulatory light chain), and a tetramethylrhodamine acceptor was attached to a reactive site in the catalytic domain (at cys 707). Fig. 8 shows the donor-lifetime in absence and presence of acceptor. There is 21% energy transfer, and using a calculated R_o of 58 Å, leads to a measured distance of 72 Å, in good agreement with the distance observed in the myosin crystal structure of 68 Å [43].

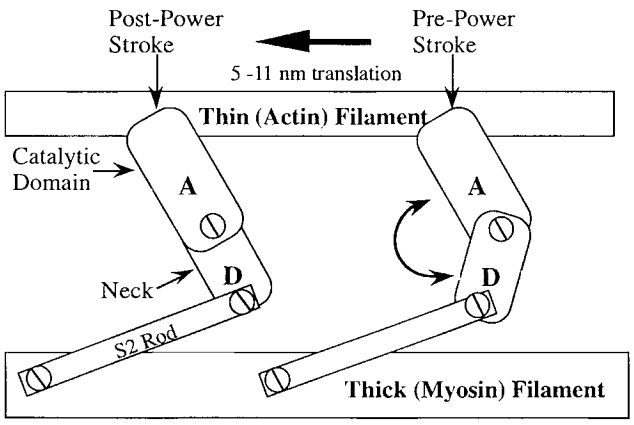

Fig. 7. Protruding from the thick filaments are myosin rods with myosin heads at the end. Conformational changes between the catalytic and neck regions of the myosin head lead to translation of the thin filament with respect to the thick filament. Detecting this neck swing is a central goal of actomyosin studies.

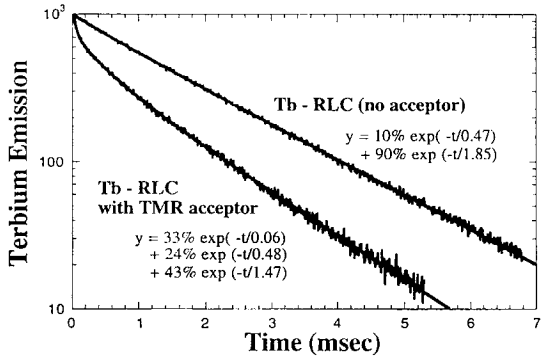

Fig. 8. With terbium labeled on the neck region (the regulatory light chain [RLC]) and the catalytic domain unlabeled, the donor-only signal is predominantly single exponential and 1.85 ms. If the catalytic domain is labeled with acceptor (TMR), then the Tb lifetime decreases due to 1.47 ms. (The 0.06 ms component is due to ringing of the detector following the excitation pulse, and the 0.48 ms component in both signals is due to a component of terbium which is quenched, perhaps due to some denatured protein.) With an R_o of 58 Å and $E = 1-1.47/1.85 = 20.5\%$, a calculated R of 72 Å is found, in good agreement with the crystal structure.

VIII. Conclusion

LRET is a powerful technique for the measurement of distances on relatively complex biomolecules. With a proper understanding of lanthanide photophysics, the underlying dipole-dipole theory relevant to FRET can be applied to LRET. LRET is relatively new, but the development of luminescent lanthanide chelates, instrumentation and measurements on model systems has been achieved. Future advances in the development of chelates, in understanding of lanthanide photophysics, and in measuring relatively long distances (>100 Å), should enable accurate measurements of distances in a wide-range of new biological systems.

Acknowledgment

The author would like to thank E. Burmeister Getz and R. Cooke, University of California, San Francisco, for collaborating on the muscle measurements. He also thanks T

Ha, Lawrence Berkeley Laboratory, for pointing out the dependence of distance-calculations on the acceptor quantum yield.

REFERENCES

[1] L. Stryer, "Fluorescence energy transfer as a spectroscopic ruler," *Annu. Rev. Biochem.*, vol. 47, pp. 819–846, 1978.

[2] R. H. Fairclough and C. R. Cantor, "The use of singlet—singlet energy transfer to study macromolecular assemblies," in *Meth. in Enzymol.*, 1978, vol. 48, pp. 347–379.

[3] C. R. Cantor and P. R. Schimmel, *Biophysical Chemistry*. San Francisco, CA: W. H. Freeman, 1980, vol. 2.

[4] B. Herman, "Resonance energy transfer microscopy," *Meth. Cell Biol.*, vol. 30, pp. 219–243, 1989.

[5] P. R. Selvin, "Fluorescence resonance energy transfer," in *Methods in Enzymology*, K. Sauer, Ed. Orlando, FL: Academic, 1995, vol. 246, pp. 300–334.

[6] R. M. Clegg, "Fluorescence resonance energy transfer," *Curr. Op. Biotechnol.*, vol. 6, pp. 103–110, 1995.

[7] ——, "Fluorescence resonance energy transfer," in *Fluorescence Imaging Spectroscopy and Microscopy*, vol. 137, *Chemical Analysis Series*, X. F. Wang and B. Herman, Eds. New York: Wiley, 1996, pp. 179–251.

[8] R. E. Dale, J. Eisinger, and W. E. Blumberg, "The orientational freedom of molecular probes," *Biophys. J.*, vol. 26, pp. 161–194, 1979.

[9] L. Stryer and R. P. Haugland, "Energy transfer: A spectroscopic ruler," in *Proc. Nat. Acad. Sci., USA*, 1967, vol. 58, pp. 719–726.

[10] T. M. Jovin and D. J. Arndt-Jovin, "Luminescence digital imaging microscopy," in *Annu. Rev. Biophys. Biophysical Chem.* Palo Alto, CA: Annual Reviews, Inc., vol. 18, 1989, pp. 271–308.

[11] ——, "FRET microscopy: Digital imaging of fluorescence resonance energy transfer. Applications in cell biology," in *Microspectrofluorimetry of Single Living Cells*, E. Kohen, J. S. Ploem, and J. G. Hirschberg, Eds. Orlando, FL: Academic, 1989, pp. 99–117.

[12] T. M. Jovin, D. J. Arndt-Jovin, G. Marriott, R. M. Clegg, M. Robert-Nicoud, and T. Schormann, "Distance, wavelength and time: The versatile 3rd dimensions in light emission microscopy," in *Optical Microscopy for Biology*, B. Herman and K. Jacobson, Eds. New York: Wiley–Liss, 1990, pp. 575–602.

[13] R. M. Clegg, "Fluorescence resonance energy transfer and nucleic acids," in *Methods in Enzymology*, D. M. J. Lilley and J. E. Dahlberg, Eds. New York: Academic, 1992, vol. 211, pp. 353–388.

[14] R. M. Clegg, A. I. Murchie, A. Zechel, and D. M. Lilley, "Observing the helical geometry of double-stranded DNA in solution by fluorescence resonance energy transfer," in *Proc. Nat. Acad. Sci., USA*, 1993, vol. 90, pp. 2994–2998.

[15] P. R. Selvin and J. E. Hearst, "Luminescence energy transfer using a terbium chelate: Improvements on fluorescence energy transfer," *Proc. Nat. Acad. Sci. USA*, vol. 91, pp. 10024–10028, 1994.

[16] P. R. Selvin, T. M. Rana, and J. E. Hearst, "Luminescence resonance energy transfer," *J. Amer. Chem. Soc.*, vol. 116, pp. 6029–6030, 1994.

[17] G. Mathis, "Rare earth cryptates and homogeneous fluoroimmunoassays with human sera," *Clin. Chem.*, vol. 39, pp. 1953–1959, 1993.

[18] ——, "Probing molecular interactions with homogeneous techniques based on rare earth cryptates and fluorescence energy transfer," *Clin. Chem.*, vol. 41, pp. 1391–1397, 1995.

[19] T. Ha, T. Enderle, D. F. Ogletree, D. S. Chemla, P. R. Selvin, and S. Weiss, "Fluorescence resonance energy transfer between a single donor and a single acceptor molecule," in *Proc. Nat. Acad. Sci.*, 1996, vol. 93, pp. 624–628.

[20] A. R. Holzwarth, "Time-resolved fluorescence spectroscopy," in *Methods in Enzymology*, vol. 246, K. Sauer, Ed. Orlando, FL: Academic, 1995, pp. 334–362.

[21] J.-C. G. Bunzli, "Luminescent probes," in *Lanthanide Probes in Life, Chemical and Earth Sciences. Theory and Practice*, B. J.-C. G. and G. R. Choppin, Eds. New York: Elsevier, 1989, pp. 219–293.

[22] E. Soini and T. Lovgren, "Time-resolved fluorescence of lanthanide probes and applications in biotechnology," *CRC Crit. Rev. in Analytical Chem.*, vol. 18, pp. 104–154, 1987.

[23] M. Li and P. R. Selvin, "Luminescent lanthanide polyaminocarboxylate chelates: The effect of chelate structure," *J. Amer. Chem. Soc.*, vol. 117, pp. 8132–8138, 1995.

[24] M. Li and P. R. Selvin, "Amine-reactive forms of a luminescent DTPA chelate of terbium and europium: Attachment to DNA and energy transfer measurements," *Bioconjugate Chem.*, vol. 8, pp. 127–132, 1997.

[25] P. R. Selvin, "Thiol-reactive luminescent lanthanide chelates," manuscript in preparation.

[26] W. D. Horrocks, Jr., and D. R. Sudnick, "Lanthanide ion probes of structure in biology. Laser-induced luminescence decay constants provide a direct measure of the number of metal-coordinated water molecules," *J. Amer. Chem. Soc.*, vol. 101, pp. 334–350, 1979.

[27] J. Bruno, W. D. Horrocks, Jr., and R. J. Zauhar, "Europium(III) luminescence and tyrosine to terbium(III) energy-transfer studies of invertebrate (octopus) calmodulin," *Biochem.*, vol. 31, pp. 7016–7026, 1992.

[28] L. Stryer, D. D. Thomas, and C. F. Meares, "Diffusion-enhanced fluorescence energy transfer," in *Annu. Rev. Biophys. Bioeng.*, vol. 11, L. J. Mullins, Ed. Palo Alto, CA: Annual Reviews, Inc., 1982, pp. 203–222.

[29] G. Marriott, M. Heidecker, E. P. Diamandis, and Y. Yan-Marriott, "Time-resolved delayed luminescence image microscopy using an europium ion chelate complex," *Biophys. J.*, vol. 67, pp. 957–965, 1994.

[30] L. Seveus, M. Vaisala, I. Hemmila, H. Kojola, G. M. Roomans, and E. Soini, "Use of fluorescent europium chelates as labels in microscopy allows glutaraldehyde fixation and permanent mounting and leads to reduced autofluorescence and good long-term stability," *Microscopy Res. Tech.*, vol. 28, pp. 149–154, 1994.

[31] A. Canfi, M. P. Bailey, and B. F. Rocks, "Multiple labeling of immunoglobulin G, albumin and testosterone with a fluorescent terbium chelate for fluorescence immunoassays," *Analyst*, vol. 114, pp. 1908–1911, 1989.

[32] R. C. Morton and E. P. Diamandis, "Steptavidin-based macromolecular complex labeled with a europium chelater suitable for time-resolved fluorescence immunoassay applications," *Anal. Chem.*, vol. 62, pp. 1841–1845, 1990.

[33] H. Takalo, V.-M. Mukkala, H. Mikola, P. Liitti, and I. Hemmila, "Synthesis of europium(III) chelates suitable for labeling of bioactive molecules," *Bioconjugate Chem.*, vol. 5, pp. 278–282, 1994.

[34] K. H. Drexhage, "Monomolecular layers and light," *Scientific Amer.*, vol. 222, pp. 108–119, 1970.

[35] D. L. Dexter, "A theory of sensitized luminescence in solids," *J. Chem. Phys.*, vol. 21, pp. 836–850, 1953.

[36] "Amersham life science catalog," 1996.

[37] A. Waggoner, "Fluorescence labeling," in *Methods in Enzymology*, K. Sauer, Ed. Orlando: Academic, 1995, vol. 246.

[38] L. Stryer, *Biochemistry*. San Francisco: W.H. Freeman, 1994.

[39] J. T. Finer, R. M. Simmons, and J. Spudich, "Single myosin molecule mechanics: Piconewton forces and nanometer steps," *Nature*, vol. 368, pp. 113–119, 1994.

[40] M. Irving, T. S. Allen, C. Sabido-David, J. S. Craik, B. Brandmeier, J. Kendrickjones, J. E. T. Corrie, D. R. Trentham, and Y. E. Goldman, "Tilting of the light-chain region of myosin during step length changes and active force generation in skeletal muscle," *Nature*, vol. 375, pp. 688–691, 1995.

[41] A. F. Huxley, "Crossbridge tilting confirmed (comment)," *Nature*, vol. 375, pp. 631–632, 1995.

[42] C. G. dos Remedios, M. Miki, and J. A. Barden, "Fluorescence resonance energy transfer measurements of distances in actin and myosin. A critical evaluation," *J. Mus. Res. Cell & Motility*, vol. 8, pp. 97–117, 1987.

[43] I. Rayment, W. R. Rypniewski, K. Schmidt-Base, R. Smith, D. R. Tomchick, M. M. Benning, D. A. Winkelmann, G. Wesenberg, and H. M. Holden, "Three-dimensional structure of myosin subfragment-1: A molecular motor," *Science*, vol. 261, pp. 50–57, 1993.

[44] P. R. Selvin, J. Jancarik, M. Li, and L.-W. Hung, "Crystal structure and spectroscopic characterization of a luminescent europium chelate," *Inorg. Chem.*, vol. 35, pp. 700–705, 1996.

Paul R. Selvin received the B.S. degree in physics from the University of Michigan, Ann Arbor, in 1983, and the Ph.D. degree in physics from the University of California, Berkeley, in 1990.

His Ph.D. research involved developing and applying spectroscopic techniques to the study of DNA dynamics. He then transferred to the Chemistry Department at Berkeley where he was a Post-Doctoral and Research Chemist from 1991 to 1995. In 1995, he joined the Lawrence Berkeley National Laboratory where he is currently a Staff Scientist in the Life Sciences Division. In the summer 1997, he will leave Berkeley to join the faculty in the Department of Physics at the University of Illinois, Urbana-Champaign.